LASER TECHNOLOGY FOR PRECISION MONOENERGETIC GAMMA-RAY SOURCE R&D AT LLNL*

M. Y. Shverdin, A. Bayramian, F. Albert, S.G. Anderson, S. M. Betts, T. S. Chu, R. R. Cross, D. J. Gibson, R. Marsh, M. Messerly, H. Phan, M. Prantil, S. Wu, C. Ebbers, R. D. Scarpetti, F. V. Hartemann, C. W. Siders, D. P. McNabb, R. E. Bonanno, and C. P. J. Barty, Lawrence Livermore National Lab, Livermore, CA, 94550, USA

Abstract

Generation of mono-energetic, high brightness gamma-rays requires state of the art lasers to both produce a low emittance electron beam in the linac and high intensity, narrow linewidth laser photons for scattering with the relativistic electrons. Here, we overview the laser systems for the 3^{rd} generation Monoenergetic Gamma-ray Source (MEGa-ray) currently under construction at Lawrence Livermore National Lab (LLNL). We also describe a method for increasing the efficiency of laser Compton scattering through laser pulse recirculation. The fiber-based photoinjector laser will produce 50 μJ temporally and spatially shaped UV pulses at 120 Hz to generate a low emmittance electron beam in the X-band RF photoinjector. The interaction laser generates high intensity photons that focus into the interaction region and scatter off the accelerated electrons. This system utilizes chirped pulse amplification and commercial diode pumped solid state Nd:YAG amplifiers to produce 0.5 J, 10 ps, 120 Hz pulses at 1064 nm and up to 0.2 J after frequency doubling. A single passively mode-locked Ytterbium fiber oscillator seeds both laser systems and provides a timing synch with the linac.

INTRODUCTION

Emerging monoenergetic gamma-ray (MEGa-ray) sources enable high impact technological and scientific missions such as isotope-specific nuclear resonance fluorescence [1, 2], radiography of low density materials [3], precision nuclear spectroscopy [4], medical imaging and treatment [5, 6], and tests of quantum chromodynamics [7]. Demonstrated Compton-scattering based γ-ray sources have produced either tunable, long pulse duration radiation [8, 9, 10] or subpicosecond γ-rays for dynamic experiments [11, 12, 13]. A recently completed, 2^{nd} generation MEGa-ray source, T-REX, at LLNL utilized an existing S-band linac and energetic picosecond interaction laser pulses to produce a record peak brilliance of 1.5x10^{15} photons/mm^2/mrad^2/s/0.1% bandwidth (BW) at 478 keV [3].

We are currently constructing a 3^{rd} generation MEGa-ray source, termed VELOCIRAPTOR, at LLNL. The new high brightness machine is designed to produce up to 2 MeV γ-rays with a peak flux of 10^{19} photons/sec, an average flux of 10^{10} photons/sec, and an energy spread of 0.5%. VELOCIRAPTOR will utilize a new, compact, high-gradient, 250 MeV X-band linac and a new, compact, high average power laser system optimized for high flux, narrow-band, tunable γ-ray generation. Here, we detail the laser technology of this MEGa-ray source.

* This work performed under the auspices of the U.S. Department of Energy by Lawrence Livermore National Laboratory under Contract DE-AC52-07NA27344.

LASER SYSTEM OVERVIEW

The VELOCIRAPTOR laser system consists of two main components: Photogun Drive Laser (PDL), which delivers spatially and temporally shaped UV pulses to RF photogun, and Interaction Laser System (ILS), which delivers, focused, high energy, picosecond duration pulses to the laser-electron interaction region (see Fig. 1). PDL and ILS are both seeded by a mode-locked and phase-locked Yb:doped fiber oscillator, which enables sub-picosecond synchronization between the generated electron bunches and the TW-class laser pulses that drive the Compton scattering interaction. Both the PDL and the ILS rely on chirped pulse amplification (CPA) to produce energetic ultrashort pulses at the output.

Fiber Front End

Essential to building a compact highly stable laser system is a fiber front end. The 10 W front-end includes a Yb:doped mode-locked oscillator, which, when compressed, produces 250 pJ, sub 100 fs, near transform limited pulses at 40.8 MHz repetition rate with a full bandwidth from 1035 nm to 1085 nm, and a chain of fiber amplifiers. A 20 nm bandwidth portion of the full spectrum centered at 1053 nm seeds the PDL; a 1 nm portion bandwidth centered at 1064 nm seeds the ILS.

The PDL fiber chain will produce over 1 mJ/pulse at 10 kHz, at the output. The pulses after the oscillator are first pre-stretched in a 100 m fiber, preamplified to 1 nJ, and then chirped to 3 ns in a bulk Offner-type bulk stretcher. A series of 3 telecom-type preamplifiers increase the pulse energy to 1 μJ at 10 kHz. Next, two bulk/hybrid 41 μm core, photonic crystal fiber amps boost the pulse energy to 100 μJ. An 85 μm core photonic crystal rod amplifier provides the final 10 dB of gain.

The ILS fiber chain will produce 30 μJ, 10 kHz pulses. A separate hyper-dispersion stretcher chirps the narrowband, 1 nm pulse to 3 ns after the oscillator. The remaining ILS

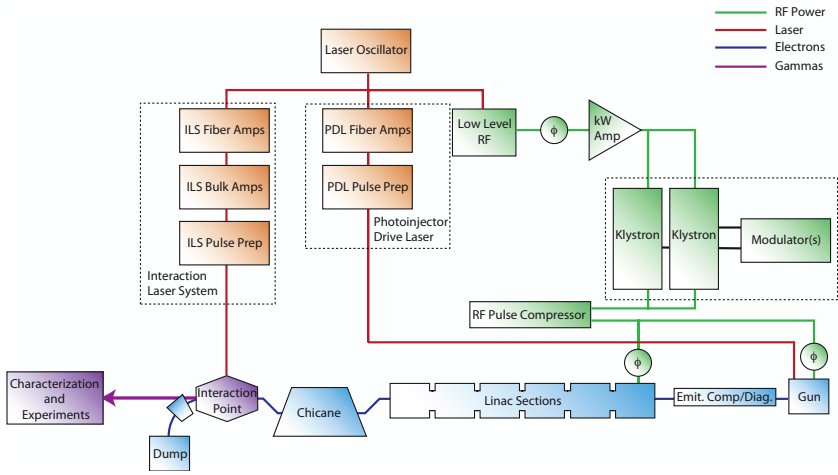

Figure 1: Schematic of VELOCIRAPTOR. Laser system (orange) is shown along with RF system (green), linac (blue) and γ-ray detection.

fiber chain contains 3 telecom-type 6 μm core fiber amps which boost the energy to 1 μJ. The final stage is a single, bulk/hybrid PZ-41 fiber amp. The 85 μm crystal rod amplifier is absent in the ILS chain, because the required pulse energy out of the fiber is lower than in PDL.

Photogun Drive Laser

The PDL will produce temporally and spatially shaped 263 nm UV pulses at the 120 Hz repetition rate on the X-band RF photocathode. The IR pulses will be compressed to 250 fs, prior to frequency conversion and temporal shaping. The bulk portion of the PDL system includes an all-reflective Offner stretcher, a folded single grating compressor, frequency quadrupling crystals, a Michelson-based temporal shaper, and gaussian to flattop spatial shaper.

The PDL pulses are chirped to 3 ns to minimize nonlinear phase accumulation. Large, 300x100 mm multilayer dielectric gratings in the stretcher and the compressor enable such long chirped pulse duration with expected throughput efficiency $>$ 75%. The all-reflective pulse stretcher is designed to minimize chromatic and geometrical phase errors, highly relevant for stretched/compressed pulse duration ratio of 15000 in the PDL. The stretcher and compressor pair are slightly mismatched to compensate for various material contributions in the system and is designed to minimize the rms residual group delay weighted by pulse bandwidth.

After pulse compression, the 250 fs, 1 mJ IR pulses are first frequency doubled and then quadrupled in two sub-millimeter thick BBO crystals. We predict 20% frequency conversion efficiency from 1ω to 4ω, primarily limited by group velocity walk-off and 2-photon absorbtion at 4ω. The UV pulses are next temporally multiplexed in a Michelson-based pulse shaper [14]. The pulse stacker generates 8 temporally delayed, orthogonally polarized, replicas of the incident pulse with femtosecond precision. The ideal shape duration is 8-10^o of the RF frequency (2 ps), with rise and fall times ($\leq 1^o$ or 200 fs). After the pulse stacker, we will use a refractive beam shaper to convert the incident gaussian to a flattop.

Compared to the prior version of PDL on T-REX, the new laser will produce 5x shorter pulses at 12x higher average power. Pulse amplification will be entirely fiber-based and scalable to kHz repetition rates.

Interaction Laser System

The diode pumped ILS will deliver 0.5 J, 10 ps pulses at 120 Hz repetition rate, at 1064 nm. To produce higher energy γ-rays, we will frequency double the output pulse and generate $\approx$200 mJ at 532 nm. CPA in commercial, diode pumped Nd:YAG bulk amplifiers will provide 43 dB of gain to the input fiber seed. Hyper-dispersion geometry enables CPA with narrowband pulses in Nd:YAG [15]. Compared to the 10 Hz flash lamp pumped laser on T-REX, diode pumping allows 12x increase in the repetition rate and average output power with improved beam quality. Design of the bulk hyper-stretcher is shown in Fig. 2. The anti-parallel grating arrangement results in 5x greater dispersion than a same size, standard Martinez stretcher/compressor. Compared to the chirped fiber Bragg grating (CFBG) used for stretching the pulse on T-REX, the bulk stretcher provides improved recompressed pulse fidelity as evidenced by the autocorrelation measurement shown in Fig. 3. The autocorrelation with CFBG was performed with the flashlamp-pumped laser. According to frequency resolved optical gating (FROG) measurements, we recompressed the pulses to near bandwidth limited, 8.3 ps FWHM duration, with 84% of the energy contained in a 20 ps bin.

The kW-class diode pumped amplifier consists of two heads (Northrop Grumman, REA series), each containing a 1 cm diameter, 14.6 cm long Nd:YAG rod. A gaussian to flattop refractive shaper modifies the seed beam profile to optimally fill the amplifier rods, maximizing extraction ef-

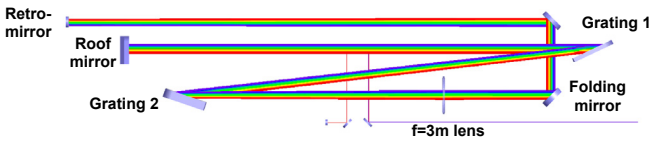

Figure 2: Hyper-dispersion stretcher provides dispersion of 7000 ps/nm in a compact 3x1 m footprint.

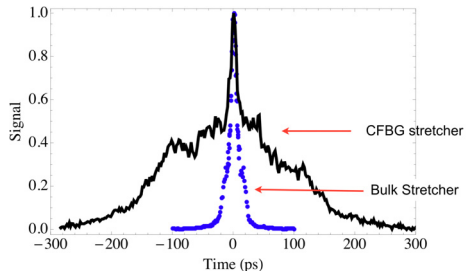

Figure 3: Autocorrelation of the compressed pulse using either CFBG (black) or bulk (blue) stretcher.

ficiency and minimizing diffractive losses. The seed beam four-passes the first amplifier head and double passes the second head producing 1 J prior to compression. A deformable mirror compensates for thermal lensing and low-order aberrations in the amplifier. The beam is relay imaged throughout the system to maintain beam quality and compensate for thermal birefringence.

After amplification, the chirped 3 ns pulse is recompressed in a compact, bulk hyper-compressor. The compressed beam will be frequency doubled in a large aperture (40x40 mm), 3.5 mm thick YCOB crystal. High thermal acceptance and favorable mechanical properties make YCOB ideal for high energy, high power frequency doubling.

Pulse Recirculation

VELOCIRAPTOR design includes an option for laser pulse recirculation. Because Compton scattering is a low efficiency process, only 1 in 10^{10} of the incident laser photons is used up in the interaction. Reusing laser photons would both, improve the conversion efficiency, and increase the generated γ-ray flux. High power, high energy, short pulse recirculation is very challenging, however. Recently, we successfully demonstrated a scheme, termed Recirculation Injection by Nonlinear Gating (RING), designed for our laser system [16].

In the simplest implementation of this technique, the incident laser pulse at the fundamental frequency enters the resonator and is efficiently frequency doubled. The resonator mirrors are dichroic, coated to transmit the 1ω light and reflect at 2ω. The upconverted 2ω pulse then becomes trapped inside the cavity. After several hundred roundtrips, the laser pulse decays primarily due to Fresnel losses at the crystal faces and cavity mirrors. Compared to active (electro-optic or accousto-optic) pulse switching, the pulse in RING scheme traverses a significantly thinner optical material, reducing nonlinear phase accumulation. Nonlinear phase accumulation limits the total number of roundtrips, because it causes beam and pulse break-up.

In an off-line demonstration, we achieved 14x average power enhancement of a 200 mJ, 10 ps pulse. By improving the spatial beam quality of the incident pulse, we expect to achieve over 30x average power enhancement, equalling our low energy (500 μJ) results obtained with a different laser system.

RING operates in a burst-pulse, multi-bunch mode, where the laser repetition frequency sets the spacing between the macro-bunches, and the cavity roundtrip time ($\approx$10 ns) determines the micro-pulse spacing within the macro-bunch. The pulse format of the photogun laser needs to match this burst mode to realize RING enhancement of the γ-ray flux. Studies of the effects of micro-bunch electron structure on beam emittance are currently under way.

In conclusion, we presented the design and the preliminary results of the laser systems for the 3^{rd} generation MEGa-ray source currently under construction at LLNL.

REFERENCES

[1] W. Bertozzi and B. Ledoux, Nucl. Instrum. Methods Phys. Res. B **241**, 820 (2005).

[2] J. Pruet, D. P. McNabb, C. A. Hagmann, F. V. Hartemann, and C. P. J. Barty, J. Appl. Phys. **99**, 123102 (2006).

[3] F. Albert, S. G. Anderson, G. A. Anderson, et. al., Opt. Lett. **35**, 354–356 (2010).

[4] N. Pietralla, Z. Berant, V. N. Litvinenko, et. al., Phys. Rev. Lett. **88**, 012502 (2001).

[5] F. E. Carroll, M. H. Mendenhall, R. H. Traeger, et. al., AM. J. ROENTGENOL. **181**, 1197–1202 (2003).

[6] M. Bech, O. Bunk, C. David, at. al., J. Synchrotron Rad. **16**, 43–47 (2009).

[7] A. I. Titov, M. Fujiwara, and K. Kawase, J. Phys. G: Nucl. Part. Phys. **32**, 1097 (2006).

[8] K. Aoki, K. Hosono, T. Hadame, et. al., Nucl. Instrum. Methods Phys. Res., Sect. A **516**, 228 – 236 (2004).

[9] T. Nakano, J. K. Ahn, M. Fujiwara, et. al., Nucl. Phys. A **684**, 71 – 79 (2001).

[10] V. N. Litvinenko, B. Burnham, M. Emamian, et. al., Phys. Rev. Lett. **78**, 4569–4572 (1997).

[11] K. Kawase, M. Kando, T. Hayakawa, et. al., Rev. Sci. Instrum. **79**, 053302 (2008).

[12] R. W. Schoenlein, W. P. Leemans, A. H. Chin, et. al., Science **274**, 236–238 (1996).

[13] D. J. Gibson, S. G. Anderson, C. P. J. Barty, et. al., AIP, 2004, vol. 11, pp. 2857–2864.

[14] C. W. Siders, J. L. W. Siders, A. J. Taylor, et. al., Appl. Opt. **37**, 5302–5305 (1998).

[15] D. N. Fittinghoff, W. A. Molander, and C. P. J. Barty, in Frontiers in Optics, Rochester, NY, (2004).

[16] I. Jovanovic, M. Shverdin, D. Gibson, C. Brown, and J. Gronberg, Nucl. Phys. B Proc. Suppl. **184**, 289 (2008).